V64

Interferometry

Lukas Bertsch
lukas.bertsch@tu-dortmund.de

Tom Troska
tom.troska@tu-dortmund.de

Date of experiment: 13.11.2023

TU Dortmund University – Faculty of Physics

Contents

1. Motivation **3**

2. Theory **3**
2.1. Coherence . . . 3
2.2. Polarization . . . 3
2.3. Contrast . . . 3
2.4. Connection with Interference and Refractive Index . . . 5
2.4.1. Refractive Index of Glass . . . 5
2.4.2. Refractive Index of Air . . . 5

3. Experimental Setup and Measurement Process **6**
3.1. Setup . . . 6
3.2. Measurement Process . . . 7
3.2.1. Alignment of the Setup . . . 7
3.2.2. Measurement of the Contrast . . . 7
3.2.3. Measurement of the Refractive Index of Glass . . . 7
3.2.4. Measurement of the Refractive Index of Air . . . 7

4. Analysis **8**
4.1. Dependence of the contrast on the polarisation angle . . . 8
4.2. Refractive index of glass . . . 8
4.3. Refractive index of air . . . 10

5. Discussion **12**

References **13**

A. Anhang **14**
A.1. Originaldaten . . . 14

1. Motivation

In this experiment we aim at determining the refractive index of air and glass by using the principles of interferometry. A Sagnac interferometer is used to achieve effects of interference.

2. Theory

When two wavefronts meet, interference phenomena can occur under certain conditions. Interference means that the waves add up according to the superposition principle. This can result in intensity maxima and minima. In the following, the physics behind interference and the connection to other physical properties like the refractive index is examined based on the example of the Sagnac interferometer.

2.1. Coherence

Two waves can interfere with other when they are coherent, meaning a constant phase relation is given. It is differentiated between temporal and spacial coherence. For the temporal coherence, the phase relation stays the same for an infinit time. Spacial coherence describes the constant phase relation regarding the spacial direction of propagation.
In reality, there will be hardly any waves that are perfectly coherent. Nevertheless, a coherence length can be identified as the distance between waves under which the waves are sufficiently coherent. The degree of coherence γ_{12} is given by

$$\gamma_{12}(\tau) = \frac{\langle E_1(t+\tau)E_2^*(t)r\rangle}{\sqrt{\langle |E_1|^2\rangle\langle |E_2|^2\rangle}}.$$

It becomes clear that the lower $|\gamma_{12}|$ the less the light is coherent with $0 \leq |\gamma_{12}| \leq 1$.

2.2. Polarization

Another important property of light is its polarization. The polarization of a light beam describes the direction in which the electric or magnetic field oscillates. Normal sunlight is unpolarized and thus has no distinguished oscillation direction of the electric or magnetic field. There are several ways to polarise light beams, for example polarization filters that only let light pass that is linearly polarized under a certain angle.
Another way to polarize light is the usage of polarizing beam splitter cubes (PBSC). When entering a PBSC, the input light beam is split into a p-polarized and a s-polarized part as depicted in Figure 1.

2.3. Contrast

The previously described interference of waves results in intensity maxima and minima. This allows for a definition of the constrast K via

$$K = \frac{I_{\max} - I_{\min}}{I_{\max} + I_{\min}}. \tag{1}$$

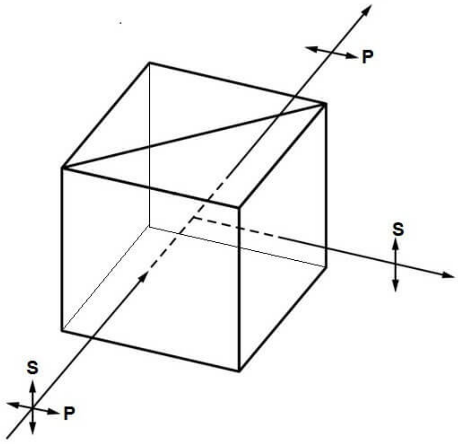

Figure 1: Visualization of the beam path in a PBSC [1].

The intensities I_{max} and I_{min} can be measured. For the derivation of a theoretical function, the intensity of the resulting wave needs to be examined. The ansatz with the superposition principle yields

$$\begin{aligned} I &\propto \langle |E_1 \cos(\omega t) + E_2 \cos(\omega t + \delta)|^2 \rangle \\ &= \langle E_1^2 \cos^2(\omega t) + 2E_1E_2 \cos(\omega t)\cos(\omega t + \delta) + E_2^2 \cos^2(\omega t + \delta) \rangle \\ &= \frac{E_1^2}{2} + E_1E_2\cos(\delta) + \frac{E_2^2}{2} \end{aligned}$$

Here, the path difference is labled as δ. For a path difference $\delta = 2\pi n$, constructive interference is achieved, whereas $\delta = (2n+1)\pi$ delivers destructive interference. Thus, the maximum and mimimum intensity calculates as

$$I_{\text{max/min}} \propto E_1^2 + E_2^2 \pm E_1E_2.$$

In case of an interferometer with a PBSC, the two light beams are polarized perpendicular to each other and the amplitudes E_1 and E_2 depend on the input polarization angle ϕ. This is the polarization angle at which the light enters the PBSC. Hence, the amplitudes result as

$$\begin{aligned} E_1 &= E_0\cos(\phi) = \sqrt{E_1 + E_2}\cos(\phi) \\ E_2 &= E_0\sin(\phi) = \sqrt{E_1 + E_2}\sin(\phi). \end{aligned}$$

With the help of this relation, the equation (2.3) simplifies to

$$I_{\text{max/min}} \propto I_{\text{Input}}(1 \pm 2\sin(\phi)\cos(\phi)). \tag{2}$$

The theoretical function for the contrast of a interferometer with a PBSC is only depended on the polarization angle of the light relative to the horizontal plane of the PBSC. It is given as

$$K = \left| \frac{(1 + 2\sin(\phi)\cos(\phi)) - (1 - 2\sin(\phi)\cos(\phi))}{(1 + 2\sin(\phi)\cos(\phi)) + (1 - 2\sin(\phi)\cos(\phi))} \right| \tag{3}$$

$$= |2\sin(\phi)\cos(\phi)|. \tag{4}$$

2.4. Connection with Interference and Refractive Index

When a light beam enters a medium, the propagation speed changes. This leads to a path difference relative to a light beam that does not propagate the medium. The discussed interference effects lead to intensity maxima and minima and the number of maxima is given as

$$M = \frac{\delta}{2\pi}. \tag{5}$$

2.4.1. Refractive Index of Glass

The path difference δ in glass is given as

$$\delta(\theta) = \frac{2\pi}{\lambda_{\text{vac}}} T \frac{n-1}{2n} \theta^2.$$

The thickness of the glass is named as T, λ_{vac} describes the wavelength in a perfect vacuum and θ is the angle of the glass in the beam path. The formula can be specialized for the case of two light beams entering the glass at different angles $\theta_1 = -\theta_2$. The path difference is then calculated as

$$\delta(\theta) = \frac{2\pi}{\lambda_{\text{vac}}} T \frac{n-1}{2n} ((\theta + \theta_1)^2 - (\theta + \theta_2)^2) \tag{6}$$

With the help of the two equations (5) and (6) the refractive index of glass yields as

$$n = \frac{1}{1 - \frac{M\lambda_{\text{vac}}}{2T\theta\theta_1}}. \tag{7}$$

2.4.2. Refractive Index of Air

The calculation of the refractive index of air is performed similarilly to the previous calculation of the refractive index of glass. Here, the path difference is given as

$$\delta = \frac{2\pi}{\lambda_{\text{vac}}} (n-1) T. \tag{8}$$

Again, the refractive index is calculated with the help of the equations (5) and (8) and reads as

$$n = \frac{M\lambda_{\text{vac}}}{T} + 1. \tag{9}$$

Apart from that, the Lorentz-Lorenz law can be used to connect the refractive index to the polarizability of a gas:

$$\frac{n^2 - 1}{n^2 + 1} = \frac{Ap}{RT}. \tag{10}$$

The universal gas constant R, the temperature T, the pressure p and the molrefraction A are needed to perform a calculation of the refractive index.

3. Experimental Setup and Measurement Process

For the measurement of the refractive index of glass and air a Sagnac interferometer is used. Its setup and the measurement process used is explained in this section.

3.1. Setup

The main feature of the Sagnac interferometer is the fact that both light beams travel the same path but in different directions. A schematic layout of a Sagnac interferometer is depicted in Figure 2. The input light beam is reflected by adjustable mirrors and passes

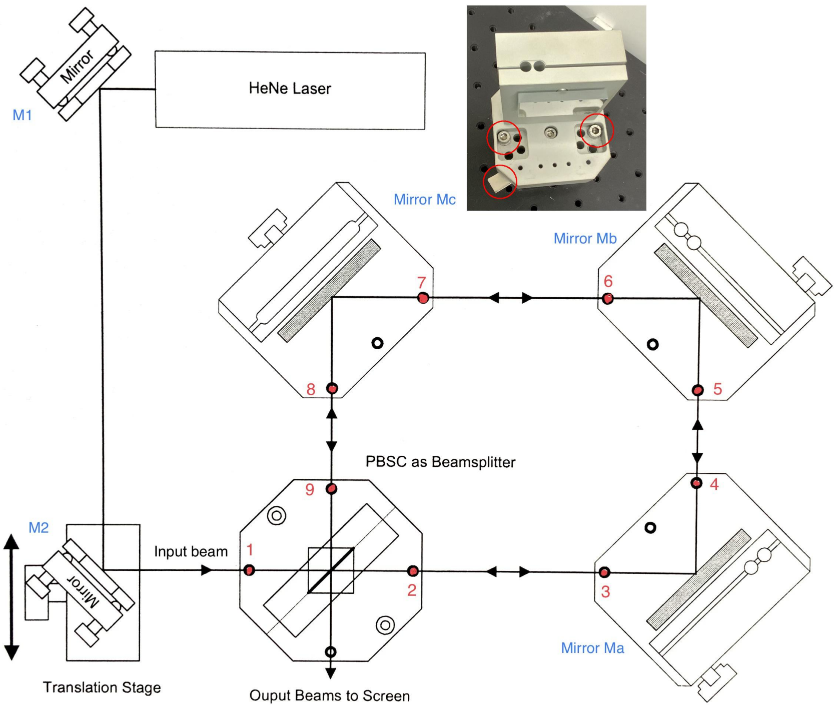

Figure 2: Layout of the Sagnac interferometer used in this experiment. The light beam is directed through the setup using several mirrors and is splitted into two beams at the PBSC [3].

through an adjustable polarization filter before it enters the PBSC. Here, it is split into its s- and p-polarized parts. The single beams are directed clockwise and counterclockwise through the setup. Since the two light beams are differently polarized, a polarization filter is placed behind the output of the PBSC to filter out the parts of the beams that can interfer. Before the intensity of the light beam is measured, it is split into the s- and p-polarized parts again using a PBSC. The intensity of the s- and p-polarized parts is determined using photodiods. The use of two photodiodes allows the implementation of a differential amplifier. The signal of the amplifier is connected to the read-out electronics that measure the number of intensity maxima.

3.2. Measurement Process

3.2.1. Alignment of the Setup

Before the actual measurements can start, the setup needs to be properly aligned. The light beams need to be spacially separated and adjusted so that they recombine at the PBSC. It needs to be ensured that the beams are directed in one plane and do not diverge.
With the help of the adjustment screws at the mirrors, the setup is adjusted to achieve broad regions of destructive interference to maximize the contrast.

3.2.2. Measurement of the Contrast

Once the interferometer is all aligned, the contrast is measured. Therefor, a piece of glass is place into both beam paths. The optical instrument used here is tilted by 10° for one beam and $-10°$ for the other. The mount for this instrument can be rotated with a set screw.
The aim is to measure the contrast as a function of the polarization angle of the first polarization filter. A plexiglass hood covers the setup to suppress effects of reflecion at air molecules. Finally, the intensity of the maxima and minima is measured at one photodiode using a voltmeter. The maxima and minima are set by turning the adjusting screw on the glass holder ever so slightly that the voltage maximizes or minimizes. This process is repeated three times for an angle range of $0° \leq \phi \leq 180°$.

3.2.3. Measurement of the Refractive Index of Glass

For the measurement of the refractive index of glass the read-out electronics that measure the number of maxima is used. The glass holder is rotated slowly for an angle range of $0° \leq \theta \leq 8°$ and the number of maxima is counted. This is performed ten times to reduce statistical uncertainties.

3.2.4. Measurement of the Refractive Index of Air

The refractive index of air is measured in a similar way. A cell that can be evacuated is placed in one of the light beams. By slowly increasing the cell pressure the intensity maxima are again counted by the read-out electronics. The cell is evacuated and repressurized five times.

4. Analysis

4.1. Dependence of the contrast on the polarisation angle

At first the dependence of the contrast on the polarisation angle ϕ is analysed. The measurements listed in Table 1 show the minimum and maximum intensity of the lasers interference for different polarisation angles ϕ.

Table 1: Measurements for the polarisation angle dependence of the contrast K.

ϕ / °	I_{min1} / V	I_{max1} / V	I_{min2} / V	I_{max2} / V	I_{min3} / V	I_{max3} / V
0	1.60	1.75	1.57	1.77	1.63	1.78
15	0.97	1.57	0.94	1.49	0.95	1.54
30	0.51	1.28	0.52	1.27	0.53	1.30
45	0.39	1.31	0.40	1.34	0.40	1.36
60	0.53	1.74	0.54	1.78	0.53	1.76
75	0.96	2.23	0.97	2.13	0.98	2.21
90	1.87	2.05	1.97	2.41	2.01	2.24
105	1.81	3.10	1.78	3.22	1.84	3.53
120	1.31	4.30	1.35	4.23	1.41	4.47
135	1.15	5.06	1.23	4.78	1.21	5.05
150	1.39	4.44	1.44	4.32	1.47	4.54
165	1.65	3.16	1.69	3.19	1.73	3.33
180	1.66	1.87	1.64	1.82	1.80	2.01

In order to compute the contrast K, Equation 1 is applied for each measurement series. After that, the average values and the standard deviations of the three measurements are calculated. The corresponding datapoints are shown in Figure 3. The theory law of the angle dependence is given by Equation 4. Here, a function of the form

$$K = 2K_0 \cdot |\sin(\phi - \delta)\cos(\phi - \delta)|$$

is fitted to the data points. The offset δ is used to compensate for deviations in the experimental setup. The fitparameters follow as

$$K_0 = 0.57 \pm 0.01 \qquad \delta = (3.23 \pm 0.58)°$$

using the *python* extension *scipy* [4]. The resulting fit function is also displayed in Figure 3. For the following measurements the polarisation angle is set to 45°.

4.2. Refractive index of glass

For the determination of the refractive index of glass the double glass holder is placed in the two beams. The two glass panes are already tilted by an angle $\Theta_0 = \pm 10°$. Using

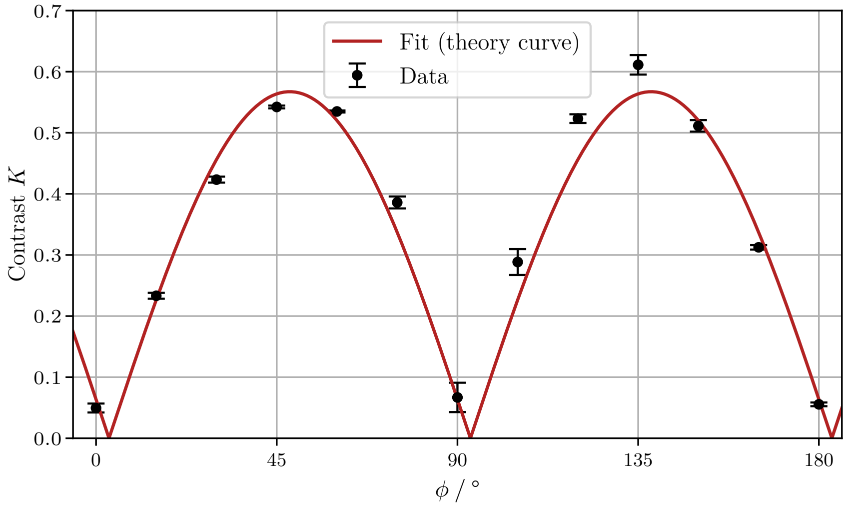

Figure 3: Averaged measurements of the contrast K against the polarisation angle ϕ and fit using *scipy* [4].

the equations (5) and (6) the number of maxima passing the center of the interference spectrum is given by

$$M = \frac{\Delta\phi_+ + \Delta\phi_-}{2\pi}$$

where $\Delta\phi_\pm$ is the phase shift induced by the glass panes tilted by $\pm 10°$. This expression can be simplified to

$$M = \frac{2T}{\lambda} \cdot \frac{n-1}{n} \cdot \Theta_0 \theta \tag{11}$$

where $\lambda = 632.99\,\mathrm{nm}$ is the wavenlength of the laser and $T = 1\,\mathrm{mm}$ is the thickness of the glass panes. The number of measured maxima is again averaged over the ten measurement series. The values are shown in Table 2. The experimental value of the

Table 2: Measurements of the maxima M passing the center of the interference spectrum and tilt angle θ.

θ	M_1	M_2	M_3	M_4	M_5	M_6	M_7	M_8	M_9	M_{10}	$\overline{M}$
2	6	6	6	6	5	6	6	6	7	6	6.00 ± 0.45
4	12	13	12	13	12	12	12	12	13	12	12.30 ± 0.46
6	19	20	19	20	18	19	18	20	20	19	19.20 ± 0.75
8	25	26	25	26	24	25	25	26	26	25	25.30 ± 0.64

refractive index of glass follows from a linear fit of Equation 11 to the datapoints. The datapoints and the fit are shown in Figure 4. The resulting value is $n_{\mathrm{glass}} = 1.484 \pm 0.008$.

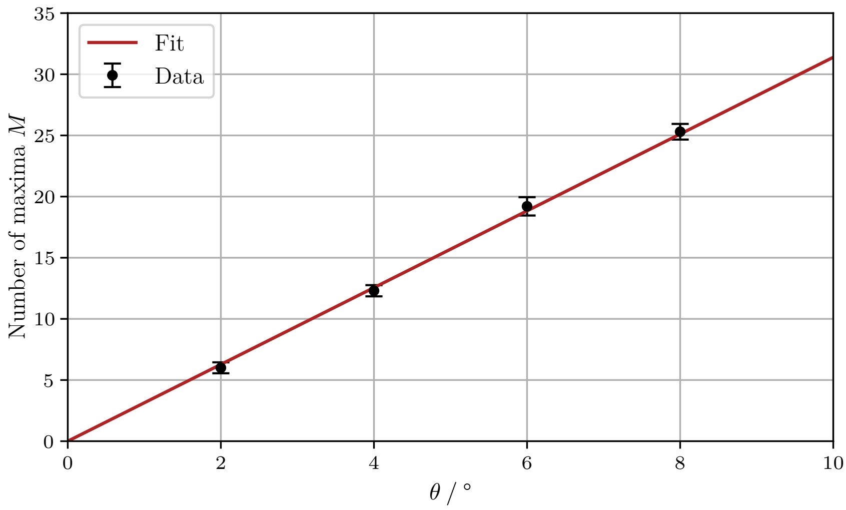

Figure 4: Averaged measurements of the number of maxima $\overline{M}$ against the tilt angle θ and fit using *scipy* [4].

4.3. Refractive index of air

To determine the refractive index of air, the measurements listed in Table 3 are used. Again the average over the five measurement series is calculated. Using Equation 9 and the length $L = (100.0 \pm 0.1)$ mm of the air chamber the corresponding refractive indices of air can be calculated at each pressure value. The resulting refractive indices are also listed in Table 3 and are shown against the pressure in Figure 5. From these values, the refractive index of air at standard atmosphere ($T = 15\,°\mathrm{C}$, $p = 1013\,\mathrm{hPa}$) can be optained. The Lorentz-Lorenz law (Equation 10) can be approximated for $n \approx 1$ as

$$n = \frac{3}{2}\frac{Ap}{RT} + 1.$$

Using this approach, the experimentally determined values of the refractive index in Figure 5 are fitted with a linear function

$$n(p, T = T_0) = \frac{3}{2}\frac{p}{RT_0} \cdot a + b$$

where a and b are the free parameters of the fit and $T_0 = 22.2\,°\mathrm{C} = 295.35\,\mathrm{K}$ is the measured room temperature. The fit parameters determined using scipy [4] follow as

$$a = (4.38 \pm 0.02) \times 10^{-4} \qquad b = 1 + (3 \pm 66) \times 10^{-8}.$$

The experimental value of the refractive index of air at standard atmosphere then reads $n_{\mathrm{exp}} = 1 + (27.05 \pm 0.13) \times 10^{-5}$.

Table 3: Measurements of the maxima M passing the center of the interference spectrum and pressure p in the air chamber. The refractive indices are displayed for the averaged value for each pressure.

p / mbar	M_1	M_2	M_3	M_4	M_5	$(\overline{n}-1)$ / 10^{-5}
8	0	0	0	0	0	0
50	2	2	2	2	2	1.27
100	4	4	4	4	4	2.53
150	6	6	6	7	6	3.92 ± 0.25
200	8	9	9	9	9	5.57 ± 0.25
250	10	11	11	11	11	6.84 ± 0.25
300	13	13	13	13	13	8.23 ± 0.01
350	15	15	15	15	15	9.49 ± 0.01
400	17	17	17	17	17	10.76 ± 0.01
450	19	19	19	19	19	12.03 ± 0.01
500	21	21	21	21	21	13.29 ± 0.01
550	23	23	23	23	23	14.56 ± 0.01
600	25	25	25	25	25	15.82 ± 0.02
650	27	28	28	27	27	17.34 ± 0.31
700	29	30	30	30	30	18.86 ± 0.25
750	32	32	32	32	32	20.26 ± 0.02
800	34	34	34	34	34	21.52 ± 0.02
850	36	36	36	36	36	22.79 ± 0.02
900	38	38	38	38	38	24.05 ± 0.02
950	40	40	40	40	40	25.32 ± 0.03
981	41	41	41	41	41	25.95 ± 0.03

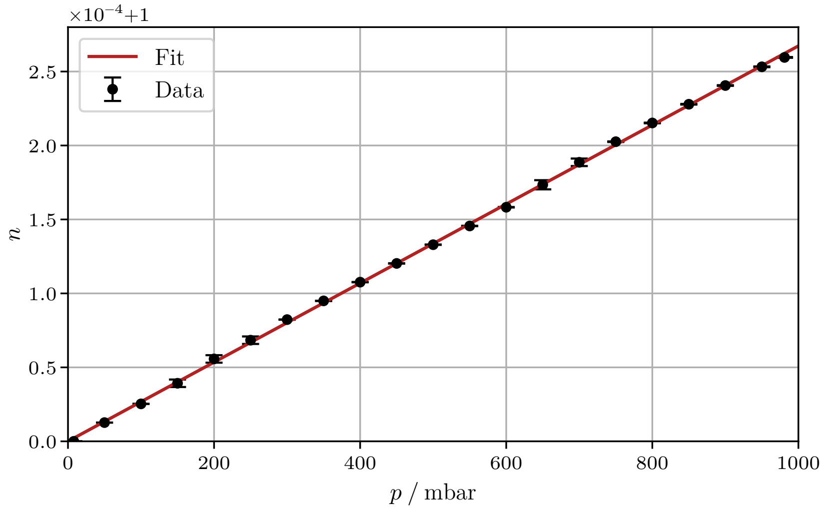

Figure 5: Calculated refractive index of air against measured pressure and linear fit using *scipy* [4].

5. Discussion

The dependence of the contrast on the polarisation angle showed good agreement between the expected theory curve and the observed data. An angle offset of $\delta = (3.23 \pm 0.58)°$ was observed compared to the theory which could possibly be explained by a constant offset on the scale of the polariser or other deviations in the experimental setup. The maximum contrast reaches a value of $K_0 = 0.57 \pm 0.01$ where the ideal contrast would be $K = 1$. This could hint to a suboptimal alignment.
The refractive index of glass was determined to be $n_{\text{glass, exp}} = 1.484 \pm 0.008$. In the literature the value is given by $n_{\text{glass, theory}} \approx 1.515$ [2], but many different glass types exist with different refractive indices. The relative deviation of the experimental value is $\Delta_{\text{rel}}(n_{\text{glass}}) = 2\,\%$. Considering the general experimental uncertainties and the fact, that the exact composition of the glass panes used in the experiment is unknown, the refractive index of glass was determined with sufficient precision.
Lastly, the refractive index of air at standard atmosphere (15 °C, 1013 hPa) was determined as $n_{\text{air, exp}} = 1.000\,270\,5 \pm 0.000\,001\,3$. The literature value is $n_{\text{air, theory}} = 1.00027653$ [2] which implies a deviation of $\Delta_{\text{rel}}(n_{\text{air}}) < 0.001\,\%$. The small deviation could e.g. be caused by humidity in the air which was neglected for the theory value. Therefore, the refractive index of air was determined precisely. All in all, the refractive indices were determined successfully, but a more careful alignment of the Sagnac-interferometer could lead to a higher contrast which may increase precision.

References

[1] *Polarisierende Strahlteilerwürfel*. Artifex Engineering GmbH Co KG. URL: https://artifex-engineering.com/de/optiken/strahlteiler/polarisierende-strahlteilerwuerfel/ (visited on 16/11/2023).

[2] Mikhail Polyanskiy. *Refractive Index Database*. URL: https://refractiveindex.info/?shelf=glass&book=BK7&page=SCHOTT (visited on 15/11/2023).

[3] *V64 - Interferometry*. TU Dortmund.

[4] Pauli Virtanen et al. 'SciPy 1.0: Fundamental Algorithms for Scientific Computing in Python'. In: *Nature Methods* 17 (2020), pp. 261–272. DOI: 10.1038/s41592-019-0686-2.

A. Anhang

A.1. Originaldaten